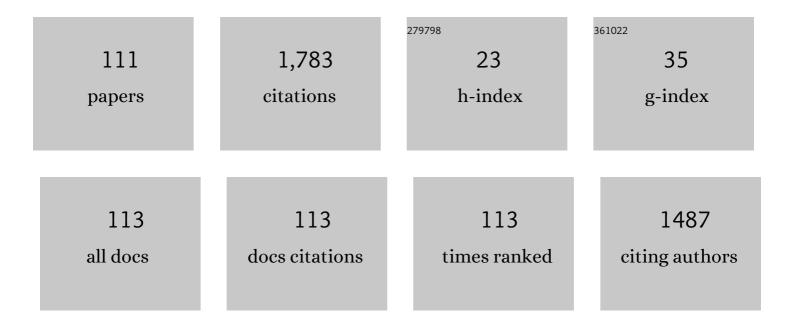
List of Publications by Year in descending order

Source: https://exaly.com/author-pdf/9554953/publications.pdf Version: 2024-02-01



ΙΙΝΙ SΗΛΟ ΗΙΙΛ

#	Article	IF	CITATIONS
1	High energy and insensitive explosives based on energetic porous aromatic frameworks. Nano Research, 2022, 15, 1698-1705.	10.4	9
2	Construction of a physically cross-linked carrageenan/chitosan/calcium ion double-network hydrogel for 3-Nitro-1, 2, 4-triazole-5-one removal. Journal of Hazardous Materials, 2022, 424, 127510.	12.4	21
3	MXene hybrid polyvinyl alcohol flexible composite films for electromagnetic interference shielding. Applied Surface Science, 2022, 578, 152007.	6.1	36
4	Bandgap Engineering for Photocatalytic Polymerization of 3, 4â€Ethylenedioxythiophene (EDOT) over Cs <sub>3</sub> Bi <sub>x</sub> Sb <sub>(2â€x)</sub> Br <sub>9</sub> Inverse Opals. ChemCatChem, 2022, 14, .	3.7	6
5	The influence of temperature environmental on performance of HNIW/FOX-7 based PBXs. Scientific Reports, 2022, 12, 4988.	3.3	0
6	Improved corrosion resistance and thermal stability of insensitive NTO explosives by MXene modification in the presence of non-covalent bonds. New Journal of Chemistry, 2022, 46, 9389-9396.	2.8	1
7	Fabrication of hydrophobic AlCoCrFeNi high-entropy alloy and superior corrosion resistance to NTO aqueous solution. Journal of Alloys and Compounds, 2022, , 165394.	5.5	4
8	Thermal decomposition kinetics and thermal hazards simulation of sodium and rubidium 3,3′-dinitrimino-5,5′-bis(1H-1,2,4-triazole). Journal of Thermal Analysis and Calorimetry, 2021, 146, 717-724.	3.6	0
9	Thermal safety assessment and thermo-kinetic parameters of 5,5′-dinitramino-3,3′-bi[1,2,4-triazolate] carbohydrazide salt (CBNT). Journal of Thermal Analysis and Calorimetry, 2021, 144, 647-655.	3.6	6
10	The influences of plasticizer B2 mass fraction on the performances of CAB / B2 polymer composite materials: Combining experiments and simulations. Journal of Vinyl and Additive Technology, 2021, 27, 36-46.	3.4	0
11	Polymer-based lightweight materials for electromagnetic interference shielding: a review. Journal of Materials Science, 2021, 56, 6549-6580.	3.7	93
12	Strategies to Get Drugs across Bladder Penetrating Barriers for Improving Bladder Cancer Therapy. Pharmaceutics, 2021, 13, 166.	4.5	17
13	Transmucosal Delivery of Self-Assembling Photosensitizer–Nitazoxanide Nanocomplexes with Fluorinated Chitosan for Instillation-Based Photodynamic Therapy of Orthotopic Bladder Tumors. ACS Biomaterials Science and Engineering, 2021, 7, 1485-1495.	5.2	12
14	Molecular design of energetic tetrazine-triazole derivatives. Journal of Molecular Modeling, 2021, 27, 98.	1.8	3
15	Preparation of copper ferrite by sol–gel method and the synergistic catalytic for the thermal decomposition of ammonium perchlorate. Journal of Sol-Gel Science and Technology, 2021, 98, 559-567.	2.4	16
16	Thermal decomposition mechanism study of 3-nitro-1,2,4-triazol-5-one (NTO): Combined TG-FTIR-MS techniques and ReaxFF reactive molecular dynamics simulations. Fuel, 2021, 295, 120655.	6.4	44
17	Initial Decomposition Mechanism of 3-Nitro-1,2,4-triazol-5-one (NTO) under Shock Loading: ReaxFF Parameterization and Molecular Dynamic Study. Molecules, 2021, 26, 4808.	3.8	14
18	Shock Initiation Investigation of a Pressed Trinitrotoluene Explosive. Propellants, Explosives, Pyrotechnics, 2021, 46, 1717.	1.6	2

#	Article	IF	CITATIONS
19	Facile mass preparation and characterization of Al/copper ferrites metastable intermolecular energetic nanocomposites. RSC Advances, 2021, 11, 7633-7643.	3.6	10
20	Reactive molecular dynamics simulation of thermal decomposition for nano-FOX-7. Applied Physics A: Materials Science and Processing, 2021, 127, 1.	2.3	8
21	Effects of Crystallinity on the Photocatalytic Polymerization of 3,4-Ethylenedioxythiophene over CsPbBr3 Inverse Opals. Catalysts, 2021, 11, 1331.	3.5	4
22	Preparation and thermal properties study of HNIW/FOX-7 based high energy polymer bonded explosive (PBX) with low vulnerability to thermal stimulations. Journal of Energetic Materials, 2020, 38, 83-97.	2.0	12
23	Preparation and performances characterization of HNIW/NTO-based high-energetic low vulnerable polymer-bonded explosive. Journal of Thermal Analysis and Calorimetry, 2020, 139, 3589-3602.	3.6	17
24	Thermal behavior, compatibility study and safety assessment of diammonium 5,5′-bistetrazole-1,1′-diolate (ABTOX). Journal of Thermal Analysis and Calorimetry, 2020, 139, 1771-1777.	3.6	17
25	A molecular dynamics study and detonation parameters calculation of 5,5'-dinitramino-3,3'-bi[1,2,4-triazolate] carbohydrazide salt (CBNT) and its PBXs. Journal of Energetic Materials, 2020, 38, 283-294.	2.0	5
26	Solubilities of 2,6â€Diaminoâ€3,5â€dinitropyrazineâ€1â€oxide in the Binary Mixtures of DMSO+H 2 O, DMF+H 2 and NMP+H 2 O in the Temperature Range from 293.15 to 323.15â€K under the Atmospheric Pressure. Propellants, Explosives, Pyrotechnics, 2020, 45, 503-508.	0 1.6	5
27	Synthesis of a Series of Dual-Functional Chelated Titanate Bonding Agents and Their Application Performances in Composite Solid Propellants. Molecules, 2020, 25, 5353.	3.8	3
28	Thermal decomposition and thermal kinetic simulation of ammonium 3,3′-dinitrimino-5,5′-bis(1H-1,2,4-triazole). Journal of Thermal Analysis and Calorimetry, 2020, 146, 911.	3.6	2
29	Density Functional Theory (DFT) Study on the Structures and Energetic Properties of Isomers of Tetranitro-bis-1,2,4-triazoles. ACS Omega, 2020, 5, 19464-19468.	3.5	10
30	Chemical synthesis of chitosan-mimetic polymers <i>via</i> ring-opening metathesis polymerization and their applications in Cu <sup>2+</sup> adsorption and catalytic decomposition. Polymer Chemistry, 2020, 11, 6688-6700.	3.9	1
31	Organic-Inorganic Artificial Ion Channel Polyvinylidene Fluoride Membranes for Controllable Selectivity Transport of Alkali Metal Cations. Membranes, 2020, 10, 174.	3.0	1
32	Design and properties of N,N'-linked bis-1,2,4-triazoles compounds as promising energetic materials. Journal of Molecular Modeling, 2020, 26, 130.	1.8	1
33	Reactive molecular dynamics simulations on the thermal decompositions and oxidations of TKX-50 and twinned TKX-50. CrystEngComm, 2020, 22, 2593-2600.	2.6	24
34	A Facile Approach to Carbon Dotsâ€Mesoporous Silica Nanohybrids and Their Applications for Multicolor and Twoâ€Photon Imaging Guided Chemo″Photothermal Synergistic Oncotherapy. ChemNanoMat, 2020, 6, 953-962.	2.8	12
35	Study on Cellulose Acetate Butyrate/Plasticizer Systems by Molecular Dynamics Simulation and Experimental Characterization. Polymers, 2020, 12, 1272.	4.5	16
36	Preparation of chitosan and carboxymethylcelluloseâ€based polyelectrolyte complex hydrogel via SDâ€Aâ€SGT method and its adsorption of anionic and cationic dye. Journal of Applied Polymer Science, 2020, 137, 48980.	2.6	26

#	Article	lF	CITATIONS
37	Decompression Process of Glycerol Shock Treatment Can Overcome Endo-Lysosomal Barriers for Intracellular Delivery. ACS Omega, 2020, 5, 33133-33139.	3.5	1
38	Pressure characteristics and safety performance of TKX-50 decomposition in confined space. Journal of Energetic Materials, 2019, 37, 1-11.	2.0	11
39	Measurement and Correlation of Solubilities of 5,5′-Dinitramino-3,3′-bi[1,2,4-triazolate] Carbohydrazide Salt (CBNT) in Various Pure Solvents and a Binary Mixture (Dimethyl Sulfoxide + Water) from 298.15 to 343.15 K. Journal of Chemical & Engineering Data, 2019, 64, 3874-3881.	1.9	6
40	Theoretical study on the weak interaction and energy performance of nitroformate salts and nitroformate-based propellant formulations. Journal of Molecular Modeling, 2019, 25, 285.	1.8	4
41	Effects of carboxymethylcellulose sodium on the morphology and properties of TKX-50, an insensitive high-energy explosive. Journal of Energetic Materials, 2019, 37, 199-211.	2.0	9
42	Preparation of chitosan-Cu2+/NH3 physical hydrogel and its properties. International Journal of Biological Macromolecules, 2019, 133, 67-75.	7.5	30
43	Molecular dynamics simulation on the morphology of 1,1-diamino-2,2-dinitroethylene (FOX-7) affected by dimethyl sulfoxide (DMSO) and temperature. Canadian Journal of Chemistry, 2019, 97, 538-545.	1.1	4
44	Effect of Sodium Alginate on the Morphology and Properties of High Energy Insensitive Explosive TKXâ€50. Propellants, Explosives, Pyrotechnics, 2019, 44, 413-422.	1.6	9
45	Investigation into the Temperature Adaptability of HNIWâ€based PBXs. Propellants, Explosives, Pyrotechnics, 2019, 44, 327-336.	1.6	6
46	Molecular dynamics investigation on the morphology of HNIW affected by the growth condition. Journal of Energetic Materials, 2019, 37, 44-56.	2.0	8
47	Theoretical study of the heats of formation, detonation properties, and bond dissociation energies of substituted bis-1,2,4-triazole compounds. Journal of Molecular Modeling, 2018, 24, 85.	1.8	9
48	Sizeâ€dependent Effect on Thermal Decomposition and Hazard Assessment of TKXâ€50 under Adiabatic Condition. Propellants, Explosives, Pyrotechnics, 2018, 43, 488-495.	1.6	16
49	Thermal stability assessment of 4,4â€2-azo-bis(1,2,4-triazolone) (ZTO) and its salts by accelerating rate calorimeter (ARC). Journal of Thermal Analysis and Calorimetry, 2018, 132, 563-569.	3.6	7
50	Thermal decomposition and safety assessment of 3,3′-dinitrimino-5,5′-bis(1H-1,2,4-triazole) by DTA and ARC. Journal of Thermal Analysis and Calorimetry, 2018, 132, 805-811.	3.6	9
51	Thermal decomposition and thermal stability of potassium 3,3′-dinitrimino-5,5′-bis(1H-1,2,4-triazole). Journal of Thermal Analysis and Calorimetry, 2018, 133, 1563-1569.	3.6	6
52	Preparation of the chitosan/poly(glutamic acid)/alginate polyelectrolyte complexing hydrogel and study on its drug releasing property. Carbohydrate Polymers, 2018, 191, 8-16.	10.2	78
53	Thermal decomposition behavior and thermal stability of DABT·2DMSO. Journal of Thermal Analysis and Calorimetry, 2018, 131, 3185-3191.	3.6	15
54	Thermal hazard assessment of TNT and DNAN under adiabatic condition by using accelerating rate calorimeter (ARC). Journal of Thermal Analysis and Calorimetry, 2018, 131, 89-93.	3.6	18

#	Article	IF	CITATIONS
55	Preparation, nonisothermal decomposition kinetics, heat capacity, and safety parameters of TKX-50-based PBX. Journal of Thermal Analysis and Calorimetry, 2018, 131, 3193-3199.	3.6	16
56	A novel cocrystal composed of CL-20 and an energetic ionic salt. Chemical Communications, 2018, 54, 13268-13270.	4.1	46
57	Preparation of the Sodium Alginate-g-(Polyacrylic Acid-co-Allyltrimethylammonium Chloride) Polyampholytic Superabsorbent Polymer and Its Dye Adsorption Property. Marine Drugs, 2018, 16, 476.	4.6	11
58	Morphology control of 3-nitro-1,2,4-triazole-5-one (NTO) by molecular dynamics simulation. CrystEngComm, 2018, 20, 6252-6260.	2.6	35
59	The primary decomposition product of TKX-50 under adiabatic condition and its thermal decomposition. Journal of Thermal Analysis and Calorimetry, 2018, 134, 2049-2055.	3.6	23
60	Molecular dynamic simulations for FOX-7 and FOX-7 based PBXs. Journal of Molecular Modeling, 2018, 24, 145.	1.8	7
61	Investigation of the effect of the CAB/A3 system on HNIW-based PBXs using molecular dynamics. Journal of Molecular Modeling, 2018, 24, 186.	1.8	1
62	Molecular dynamics simulations on miscibility, glass transition temperature and mechanical properties of PMMA/DBP binary system. Journal of Molecular Graphics and Modelling, 2018, 84, 182-188.	2.4	17
63	Miscibility, Glass Transition Temperature and Mechanical Properties of NC/DBP Binary Systems by Molecular Dynamics. Propellants, Explosives, Pyrotechnics, 2018, 43, 559-567.	1.6	3
64	The study of external growth environments on the crystal morphology of ε-HNIW by molecular dynamics simulation. Journal of Materials Science, 2018, 53, 12921-12936.	3.7	20
65	A single molecular fluorescent probe for selective and sensitive detection of nitroaromatic explosives: A new strategy for the mask-free discrimination of TNT and TNP within same sample. Talanta, 2017, 166, 228-233.	5.5	45
66	Dissolution properties of 5,5′-bistetrazole-1, 1′-dihydroxy and disodium 5,5′-bistetrazole-1, 1′-diolate dimethyl sulfoxide. Journal of Thermal Analysis and Calorimetry, 2017, 128, 615-620.	in 3.6	2
67	Molecular dynamic simulations on TKX-50/HMX cocrystal. RSC Advances, 2017, 7, 6795-6799.	3.6	30
68	Study on a novel high energetic and insensitive munitions formulation: TKX-50 based melt cast high explosive. RSC Advances, 2017, 7, 31485-31492.	3.6	18
69	Preparation, crystal structure, thermal behavior and DFT calculations of two acetyl triazolone derviatives. Journal of Molecular Structure, 2017, 1146, 32-38.	3.6	2
70	Preparation, characterization and thermal risk evaluation of dihydroxylammonium 5, 5′-bistetrazole-1, 1′-diolate based polymer bonded explosive. Journal of Hazardous Materials, 2017, 338, 208-217.	12.4	56
71	Preparation, Characterization, Thermal Evaluation and Sensitivities of TKX-50/GO Composite. Propellants, Explosives, Pyrotechnics, 2017, 42, 1104-1110.	1.6	28
72	Molecular dynamic simulations on TKX-50/RDX cocrystal. Journal of Molecular Graphics and Modelling, 2017, 74, 171-176.	2.4	31

**JIN SHAO HUA** 

#	Article	IF	CITATIONS
73	The novel compound dimethylamine-5,5′-bistetrazole-1,1′-diolate: crystal structure, thermal investigation, safety evaluation and theoretical studies. RSC Advances, 2017, 7, 18523-18528.	3.6	10
74	Thermal behavior and thermo-kinetic studies of 5,5′-bistetrazole-1,1′-diolate (1,1-BTO). Journal of Thermal Analysis and Calorimetry, 2017, 129, 1265-1270.	3.6	12
75	Dissolution thermodynamics of dihydroxylammonium 5,5′-bistetrazole-1,1′-diolate in water at TÂ=Â(298.15	,) <u>Ti </u> ETQq 3 <b>.6</b>	1 <u>1</u> 0.7843
76	Preparation and characterization of chitosan physical hydrogels with enhanced mechanical and antibacterial properties. Carbohydrate Polymers, 2017, 157, 1383-1392.	10.2	91
77	Heat effects of NTO synthesis in nitric acid solution. Journal of Thermal Analysis and Calorimetry, 2017, 128, 301-310.	3.6	8
78	Construction and Characterization of a Chitosan-Immobilized-Enzyme and β-Cyclodextrin-Included-Ferrocene-Based Electrochemical Biosensor for H2O2 Detection. Materials, 2017, 10, 868.	2.9	26
79	Preparation and Characterization of Cyclotrimethylenetrinitramine (RDX) with Reduced Sensitivity. Materials, 2017, 10, 974.	2.9	19
80	Bioresponsive Materials for Drug Delivery Based on Carboxymethyl Chitosan/Poly(γ-Glutamic Acid) Composite Microparticles. Marine Drugs, 2017, 15, 127.	4.6	37
81	Construction of a Fluorescent H2O2 Biosensor with Chitosan 6-OH Immobilized β-Cyclodextrin Derivatives. Marine Drugs, 2017, 15, 284.	4.6	5
82	Preparation of Nanofibers with Renewable Polymers and Their Application in Wound Dressing. International Journal of Polymer Science, 2016, 2016, 1-17.	2.7	58
83	Empirical Kinetics Equation of the Synthesis of NTO in Nitric Acid. Propellants, Explosives, Pyrotechnics, 2016, 41, 1085-1091.	1.6	4
84	Solubilities of Dihydroxylammonium 5,5′-Bistetrazole-1,1′-diolate in Various Pure Solvents at Temperatures between 293.15 and 323.15 K. Journal of Chemical & Engineering Data, 2016, 61, 1873-1875.	1.9	16
85	Crystal structure of 2,4,6,8,10,12-hexanitro-2,4,6,8,10,12-hexaazatetracyclo[5·5·0·05·9·03·11]dodecane hydrate, C6H8N12O13. Zeitschrift Fur Kristallographie - New Crystal Structures, 2016, 231, 491-492.	1/3. <sub>3</sub>	3
86	Triphenylamine based lab-on-a-molecule for the highly selective and sensitive detection of Zn <sup>2+</sup> and CN <sup>â^²</sup> in aqueous solution. RSC Advances, 2016, 6, 93826-93831.	3.6	17
87	Thermal stability assessment of 3,4-bis(3-nitrofurazan-4-yl)furoxan (DNTF) by accelerating rate calorimeter (ARC). Journal of Thermal Analysis and Calorimetry, 2016, 126, 1185-1190.	3.6	17
88	Crystal structure of hexaaquamagnesium(II) 5,5′-bitetrazole-1,1′-diolate, C2H12N8O8Mg. Zeitschrift Fur Kristallographie - New Crystal Structures, 2016, 231, 305-306.	0.3	0
89	Crystal structure of tetraqua((E)-4,4′-(diazene-1,2-diyl)bis(5-oxo-4,5-dihydro-1,2,4-triazol-1-ide)-κ2N:O)barium(II), C4H10N8O6Ba. Zeitschrift Fur Kristallographie - New Crystal Structures, 2016, 231, 503-504.	0.3	0
90	Crystal structure of (E)-4,4′-(diazene-1,2-diyl)bis(1-nitro-1H-1,2,4-triazol-5(4H)-one)—acetonitrile (1:1), C <sub>6</sub> H <sub>5</sub> N <sub>11</sub> O <sub>6</sub> . Zeitschrift Fur Kristallographie - New Crystal Structures, 2016, 231, 677-678.	0.3	0

#	Article	IF	CITATIONS
91	Thermal hazard assessment of 4,10-dinitro-2,6,8,12-tetraoxa-4,10-diazaisowutrzitane (TEX) by accelerating rate calorimeter (ARC). Journal of Thermal Analysis and Calorimetry, 2016, 126, 467-471.	3.6	28
92	Thermolysis, nonisothermal decomposition kinetics, calculated detonation velocity and safety assessment of dihydroxylammonium 5, 5′-bistetrazole-1, 1′-diolate. Journal of Thermal Analysis and Calorimetry, 2016, 126, 473-480.	3.6	43
93	The crystal structure and thermal analysis of ZTO and its solvent adducts. Research on Chemical Intermediates, 2016, 42, 4333-4340.	2.7	2
94	Dissolution Properties of Dihydroxylammonium 5,5Ê1-Bistetrazole-1,1Ê1-diolate and Disodium 5,5Ê1-Bistetrazole-1,1Ê1-diolate in Water. Journal of Energetic Materials, 2016, 34, 416-425.	2.0	12
95	A new multifunctional Schiff-based chemosensor for mask-free fluorimetric and colorimetric sensing of Fâ'' and CNâ''. Talanta, 2016, 152, 39-44.	5.5	39
96	Preparation, crystal structure, thermal behavior, and theoretical studies of N,N′-dinitro-4, 4′-azo-bis(1,2,4-triazolone) (DNZTO). Zeitschrift Fur Naturforschung - Section B Journal of Chemical Sciences, 2016, 71, 197-204.	0.7	4
97	Nitrogen-rich 4,4′-azo bis(1,2,4-triazolone) salts—the synthesis and promising properties of a new family of high-density insensitive materials. Dalton Transactions, 2016, 45, 3590-3598.	3.3	27
98	Molecular dynamics simulations on dihydroxylammonium 5,5′-bistetrazole-1,1′-diolate/hexanitrohexaazaisowurtzitane cocrystal. RSC Advances, 2016, 6, 4221-4226.	3.6	19
99	Evaluation of thermal hazards and thermo-kinetic parameters of N,N′-dinitro-4,4′-azo-Bis(1,2,4-triazolone) (DNZTO). Thermochimica Acta, 2016, 623, 58-64.	2.7	31
100	A simple ratiometric and colorimetric chemosensor for the selective detection of fluoride in DMSO buffered solution. Spectrochimica Acta - Part A: Molecular and Biomolecular Spectroscopy, 2016, 153, 194-198.	3.9	18
101	Kristallographie - New Crystal Structures, 2015, 230, 225-226.	0.3	2
102	Preparation, Crystal Structure and Properties of a New Crystal Form of Diammonium 5,5′â€bistetrazoleâ€1,1′â€diolate. Chinese Journal of Chemistry, 2015, 33, 1229-1234.	4.9	11
103	Unveiling the Dependence of Class Transitions on Mixing Thermodynamics in Miscible Systems. Scientific Reports, 2015, 5, 8500.	3.3	14
104	Squaramide-based lab-on-a-molecule for the detection of silver ion and nitroaromatic explosives. RSC Advances, 2015, 5, 96665-96669.	3.6	15
105	Synthesis and Characterization of 1,5â€Dinitroâ€2,6â€bis(trinitromethyl)â€3a,4a,7a,8aâ€ŧetrahydroâ€{1,4]dioxino[2,3â€d:5,6â€d′]diimidazole Propellants, Explosives, Pyrotechnics, 2013, 38, 658-664.	(DMTNDI).	. 3
106	Effects of Additives on εâ€HNIW Crystal Morphology and Impact Sensitivity. Propellants, Explosives, Pyrotechnics, 2012, 37, 77-82.	1.6	52
107	10-Formyl-2,4,6,8,12-pentanitro-2,4,6,8,10,12-hexaazatetracyclo[5.5.0.03,11.05,9]dodecane. Acta Crystallographica Section E: Structure Reports Online, 2009, 65, o3112-o3112.	0.2	3
108	Quantitative Determination of εâ€phase in polymorphic HNIW using Xâ€ray Diffraction Patterns. Propellants, Explosives, Pyrotechnics, 2008, 33, 467-471.	1.6	20

**JIN SHAO HUA** 

#	Article	IF	CITATIONS
109	Preparation of É>-HNIW by a One-Pot Method in Concentrated Nitric Acid from Tetraacetyldiformylhexaazaisowurtzitane. Propellants, Explosives, Pyrotechnics, 2007, 32, 468-471.	1.6	15
110	A novel ternary energetic compound: DAF/DNP/H2O cocrystal. Journal of Energetic Materials, 0, , 1-13.	2.0	1
111	An interesting 3D energetic metal - framework based Ag(I) ions and 3,4-diaminofurazan. Journal of Energetic Materials, 0, , 1-13.	2.0	1